

A Fast Technique for the Creation of Large-Scale High-Resolution *IRAS* (HIRES) Beam-matched Images

C. R. KERTON

Dominion Radio Astrophysical Observatory, Herzberg Institute of Astrophysics, National Research Council, P.O. Box 248,
Penticton, BC V2A 6K3, Canada; charles.kerton@nrc.ca

AND

P. G. MARTIN

Canadian Institute for Theoretical Astrophysics and Department of Astronomy, University of Toronto, 60 St. George Street,
Toronto, ON M5S 3H8, Canada; pgmartin@cita.utoronto.ca

Received 2001 March 11; accepted 2001 March 20

ABSTRACT. HIRES processing provides a significant improvement in both resolution and image quality over previous *IRAS* image products, but the characteristics of the HIRES beam make accurate comparisons between the various *IRAS* bandpasses and between HIRES data and data at other wavelengths nontrivial. We present a new, fast technique for the construction of HIRES beam-matched images that is especially well suited for the creation of large-scale (several square degree) ratio maps. Other techniques for the construction of ratio maps are discussed and compared with the new algorithm. Examples of the large-scale ratio maps that can be constructed using this new technique are presented. The algorithm's application to the construction of multiwavelength difference images and multicolor images is also demonstrated.

1. INTRODUCTION

Often one would like to create beam-matched maps of *IRAS* images in order to study the properties of the emitting grains and the incident radiation field. For example, the ratio between the *IRAS* 60 and 100 μm bands provides a measure of the equilibrium dust temperature and is often used as a proxy for the intensity of the radiation field (Helou, Ryter, & Soifer 1991). The 12 μm /100 μm ratio and 12 μm /25 μm ratio can be used to trace abundance variations in different grain populations (see, e.g., Boulanger et al. 1990; Ryter, Puget, & Pérault 1987). In order to use any such ratio image for quantitative purposes, it is important that the beam shape of the two images be well matched. The most commonly used *IRAS* image data product for such studies is the *IRAS* Sky Survey Atlas (ISSA) (Wheeler et al. 1994). With the ISSA the construction of ratio maps does not pose a significant problem since all four *IRAS* bands have been brought to a common resolution of $4' \times 5'$. Drawbacks to using these images include the presence of striping and the relatively low resolution.

HIRES processing¹ (Aumann, Fowler, & Melnyk 1990) can yield much higher spatial resolution and, with the addition of new destriping and zodiacal subtraction algorithms (Cao et al. 1996), superior image quality. However, there are a number of characteristics of the resulting images that make the creation

of an accurate ratio map nontrivial: the achieved resolution is different in each band for a given number of iterations, the beam shape varies between bands primarily because of the difference in the detector sizes, and within each band the beam shape also varies as a function of position because of the varying *IRAS* scan pattern on the sky (Cao et al. 1997; Kerton & Martin 2000). These image characteristics mean that a simple ratioing of the HIRES images is not satisfactory in the majority of cases.

Various techniques have been developed to create accurate high-resolution ratio maps with HIRES data. As will be discussed, most existing techniques for creating HIRES ratio maps tend to be time consuming and in some cases also require access to the raw *IRAS* data. The creation of a new fast technique is primarily motivated by the existence of two very large HIRES data sets that cover parts of the Galactic plane. The *IRAS* Galaxy Atlas (IGA)² (Cao et al. 1997) consists of first- and 20th iteration far-infrared (60 and 100 μm) images and ancillary files covering the entire Galactic plane between $b = \pm 4^\circ.7$. The Mid-Infrared Galaxy Atlas (MIGA)³ (Kerton & Martin 2000) is the equivalent mid-infrared data set (12 and 25 μm) covering $l = 74^\circ\text{--}148^\circ$, $b = \pm 6^\circ.5$. Both of these data sets have been incorporated as large $5^\circ.12 \times 5^\circ.12$ mosaics into the Canadian Galactic Plane

¹ HIRES images and ancillary files are available as single fields ($1^\circ\text{--}2^\circ$ in size) through the Infrared Processing and Analysis Center (IPAC).

² IGA images are available at <http://irsa.ipac.caltech.edu/applications/IGA/>.

³ MIGA images are available at <http://www.cita.utoronto.ca>.

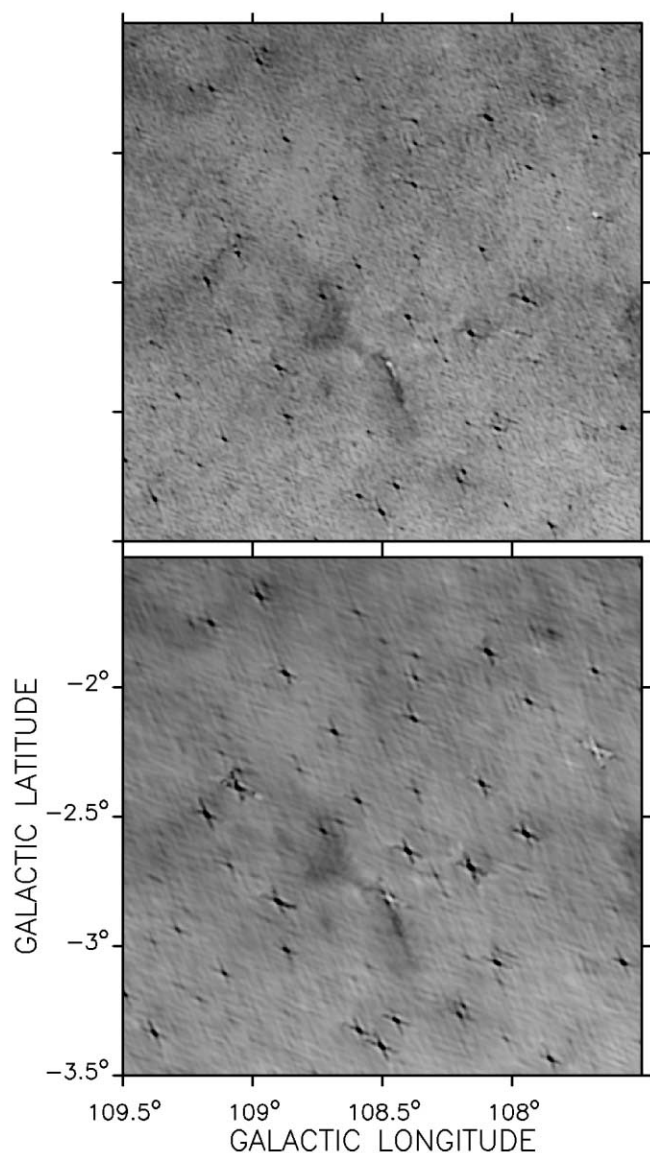


FIG. 1.—Sh 2-151 region. Figure shows a comparison of ratio maps ($12\ \mu\text{m}/25\ \mu\text{m}$) constructed using a simple division of MIGA images (*top*) and using the HIRES *IRAS* Simulator to perform cross-band beam matching (*bottom*). Images are linearly stretched from 0 (*white*) to 1 (*black*).

Survey (CGPS)⁴ (Taylor 1999) an international project that is conducting a multiwavelength [21 cm H I line, 1420 and 408 MHz continuum, CO ($J = 1-0$), and infrared] survey of the Galactic plane at a common spatial resolution of $\sim 1'$. The existence of this large uniform data set means that high-resolution studies of dust in the interstellar medium (ISM) can now be easily done over very large spatial scales.

In § 2 we review the various techniques that have been used

⁴ CGPS data are available at the Canadian Astronomy Data Centre (CADC); <http://cadcwww.hia.nrc.ca>.

to create ratio maps of HIRES images. A new technique developed specifically for the fast creation of large-scale HIRES ratio maps is presented in § 3, and the resulting ratio maps are examined in § 4. Section 5 presents some sample applications of the new technique, and conclusions are given in § 6.

2. PREVIOUS RATIO MAP CREATION TECHNIQUES

2.1. Simple Division

The similarity in the size and layout of the $12\ \mu\text{m}$ and $25\ \mu\text{m}$ detectors in the focal plane array of *IRAS* (*IRAS* Explanatory Supplement 1988) means that the resulting beam shapes are very similar and two-dimensional Gaussian fits to the beams will often agree to within the fitting errors. Beam maps showing the HIRES beam shape at various locations in the image and tables of two-dimensional Gaussian fits to the beam shape are available as part of the HIRES service at IPAC and are also included in the IGA and MIGA releases. This similarity in beam shape means that, with care, high-resolution ratio maps can be created by simply dividing the $12\ \mu\text{m}$ and $25\ \mu\text{m}$ images. Care is required because, although the beam shapes are very close, the actual beam shapes are not two-dimensional Gaussians and can vary in detail because of differences in the ratio between the point-source flux and the background level during HIRES processing between the two images (see § 4.1 of Kerton & Martin 2000 for details). As an example, Figure 1 shows two ratio maps of the region around the H II region Sh 2-151, chosen because of the unusual irregular cross-shaped beam pattern caused by the significant difference in the scan angle between the two *IRAS* coverages of the region (this effect is most noticeable at high ecliptic latitudes). The top image was constructed by simply dividing a $12\ \mu\text{m}$ image from the MIGA by the corresponding $25\ \mu\text{m}$ MIGA image, while the bottom image was constructed using the cross-band simulation technique (see § 2.4 for details) to bring the two images to a common beam shape. In general the structure shown in each image is the same, but note that the point sources are more clearly defined in the bottom image because of the matching beam shapes. For example, the feature associated with Sh 2-151 is more clearly shown to be a point source in the beam-matched image than in the simple ratio image. The lower image also has a less mottled background because of the matched beams and the slightly lower resolution. The beneficial effect of bringing the two images to the same beam shape is seen in the way that the cross-shaped beam pattern of the point sources seen in Figure 1 is undistorted in the cross-band simulator ratio image while in the simple ratio map the point sources show some nonphysical structure. Most of the point sources (stars) in the ratio image saturate and appear as black structures since they are brighter at $12\ \mu\text{m}$ than at $25\ \mu\text{m}$. The two noticeable exceptions are the point source associated with Sh 2-151 at $l = 108^\circ.5$, $b = -2^\circ.8$ and the point source at $l = 107^\circ.6$, $b = -2^\circ.24$ (the planetary nebula PK 107-2.1).

For some purposes a simple $12\ \mu\text{m}/25\ \mu\text{m}$ ratio map, such

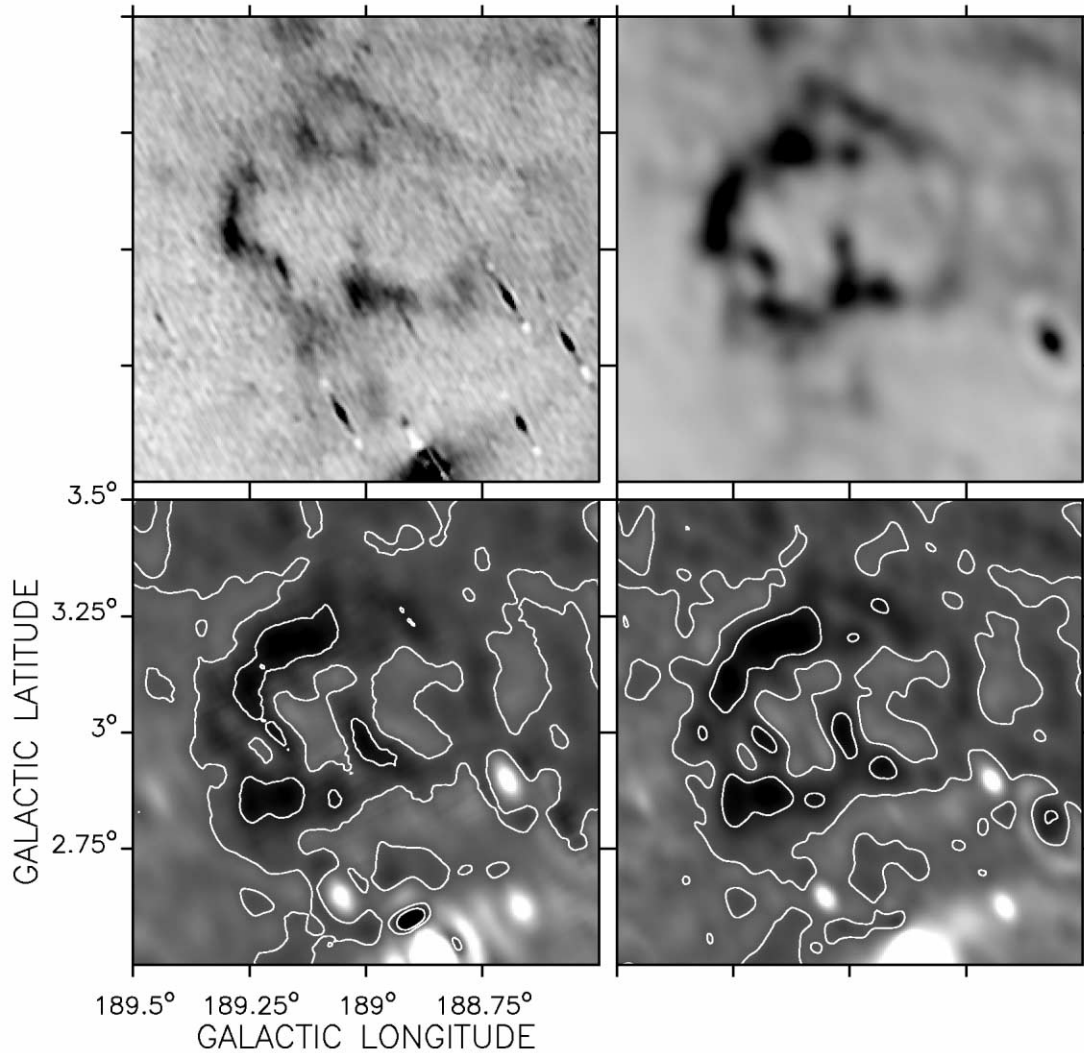


FIG. 2.—IC 443 region. Figure shows a comparison of ratio maps ($12\ \mu\text{m}/100\ \mu\text{m}$) constructed using the HIRES simulator (*bottom left*) and using the convolution technique (*bottom right*) for a region with a regular HIRES beam (linear gray scale from 0.05 to 0.14, *black to white*, with contours at 0.06 and 0.08). The top row shows the original HIRES images at $12\ \mu\text{m}$ (*left*; linear gray scale from 2.1 to $9.2\ \text{MJy sr}^{-1}$, *white to black*) and $100\ \mu\text{m}$ (*right*; linear gray scale from 10 to $120\ \text{MJy sr}^{-1}$, *white to black*).

as that shown in Figure 1, may suffice. The user needs to closely inspect the associated beam maps to determine if the beam shapes are close enough for their purposes. If so, the similar beam shape and resolution of the mid-infrared bands provides a quick and easy way to obtain high-resolution mid-infrared ratio maps. Note that any simple ratio map involving the 60 and $100\ \mu\text{m}$ bands will not be satisfactory because of the large difference in beam resolution and shape, and some form of beam matching will be desirable. This is the focus of the rest of this paper.

2.2. Convoluting to Common Lower Resolution

One simple technique that is often used is to smooth the HIRES images to a common lower resolution. For example,

Xu & Helou (1996), in their study of M31, convolve their HIRES images to a common 1.7 circular beam (their lowest original HIRES resolution) in order to construct ratio images. This technique is fast and does not require access to the original *IRAS* data (just the HIRES beam tables) but suffers from the disadvantage that one is losing much of the resolution gained by the HIRES processing. This can be a concern especially for the mid-infrared bands where one can achieve very high resolution (the original resolution of the 12 and $25\ \mu\text{m}$ images from Xu & Helou [1996] was 0.5×0.9). Over very large areas, where the beam properties are expected to change significantly, one also has to take care to use the correct convolving kernel to smooth the beams correctly. If the smoothing is very

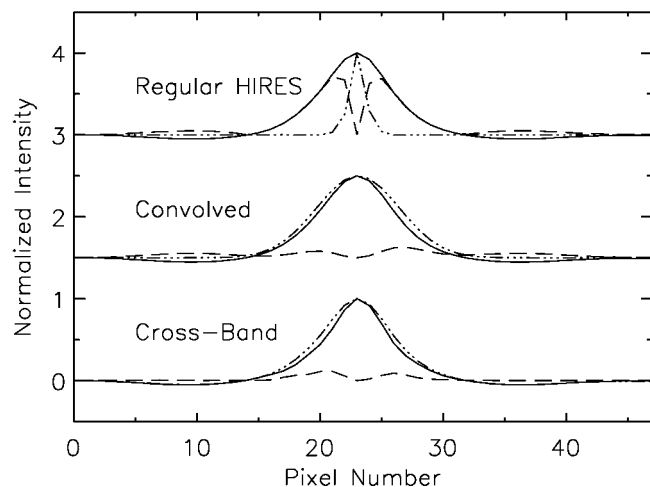


Fig. 3.—Regularly shaped HIRES beam comparison. The solid and dot-dashed lines show normalized cuts through the minor axis of a HIRES beam ($100\ \mu\text{m}$ and $12\ \mu\text{m}$, respectively) located at $l = 189^\circ$, $b = 3^\circ$. The dashed line shows the absolute difference between the two beams. The regular HIRES and convolution results have been offset by 3 units and 1.5 units, respectively.

large, this is not a major concern, but again one loses some of the advantage of using HIRES in the first place.

2.3. Variable HIRES Iteration

This technique takes advantage of the fact that the resolution achieved by HIRES processing improves as the number of iterations increases. By stopping the HIRES processing at different iterations for data at different wavelengths, one can obtain approximately matching resolution in different bands (e.g., see the Wang [1994] study of the supernova remnant IC 443). The exact beam shape can still be slightly different, so the final images are often convolved to a circular beam to reduce this effect (Wang 1994). Since this technique requires some degree of trial and error to match the beam resolution in the different bands, it is really suitable only for mapping small areas and for users that have easy access to both the raw *IRAS* archive and the HIRES processing software (YORIC).⁵

2.4. Cross-Band Simulation

The most accurate technique for matching the various HIRES beams is called cross-band simulation (Fowler & Aumann 1994). This technique makes use of the HIRES *IRAS* simulator that is part of the YORIC software package. Using this technique, if one wanted to create a ratio map of a $12\ \mu\text{m}$ image and $60\ \mu\text{m}$ image, the simulator would be used to scan the $12\ \mu\text{m}$ HIRES image with the $60\ \mu\text{m}$ detector pattern to create simulated data for the $12\ \mu\text{m}$ sky. These “observations” would then be HIRES processed as if they were $60\ \mu\text{m}$ data to create

a somewhat lower resolution version of the $12\ \mu\text{m}$ image. The same process is followed for the $60\ \mu\text{m}$ data. The final result is two images at the same resolution (in this example, each slightly poorer than the original $60\ \mu\text{m}$ HIRES resolution). The major advantage of this technique is that because the resulting beams are very well matched at every location in the image, spurious results are not introduced into the ratio maps. This technique is very time consuming since the HIRES algorithm is essentially run twice for each field that needs to be processed. Simulator images can be requested from IPAC for single fields, so a user in principle does not need direct access to the YORIC software or the *IRAS* data archive for single field images. If one is interested in creating large-scale images (such as the large mosaics that can be created with the IGA and MIGA data), then access to the YORIC software and the *IRAS* data archive is essential since large-scale mosaics cannot be created by simply patching together smaller images obtained from IPAC because of the local destriping algorithms that are used. Both the MIGA and IGA are on a common grid and were created using a special preprocessing technique that allows the easy creation of high-quality large-scale mosaics (e.g., see Cao et al. 1997 or Kerton & Martin 2000).

3. NEW ALGORITHM

Since the typical user of the MIGA, IGA, and/or CGPS data will not have access to either YORIC or the raw *IRAS* data, it is important to have a robust technique that users can apply to the data that they do have in order to construct ratio maps. The criteria used in the development of this new technique are that it should make use of only those data available to the typical user, it should be fast, and it should result in images that are close to what the cross-band simulator technique would produce.

As mentioned above, the resolution and position angle of the HIRES beam varies as a function of position over an image. As part of the standard MIGA and IGA releases two-dimensional Gaussian fits were made to the beam shape and recorded in accompanying files. This information is also available for individual HIRES processing requests. The basic assumption underlying the new ratio map technique is that the HIRES beam is well described by the two-dimensional Gaussian at the various points in the images. Clearly this assumption works best in those regions where the beam shape is “well behaved.” In the worst case, in regions of high ecliptic latitude, the beam shape can even have cross-shaped wings due to very large variations in the scan angle of the *IRAS* satellite. At these locations, while the assumption is clearly dubious, the resulting ratio maps turn out to still be useful. This is because the central part of the cross-shaped beam is still well described by the Gaussian approximation.

We describe the operation of the algorithm on a single standard HIRES field that one would obtain from either the IGA or the MIGA. In order to build up a large-scale image, one

⁵ The archive and software are available at IPAC and at the Canadian Institute for Theoretical Astrophysics (CITA).

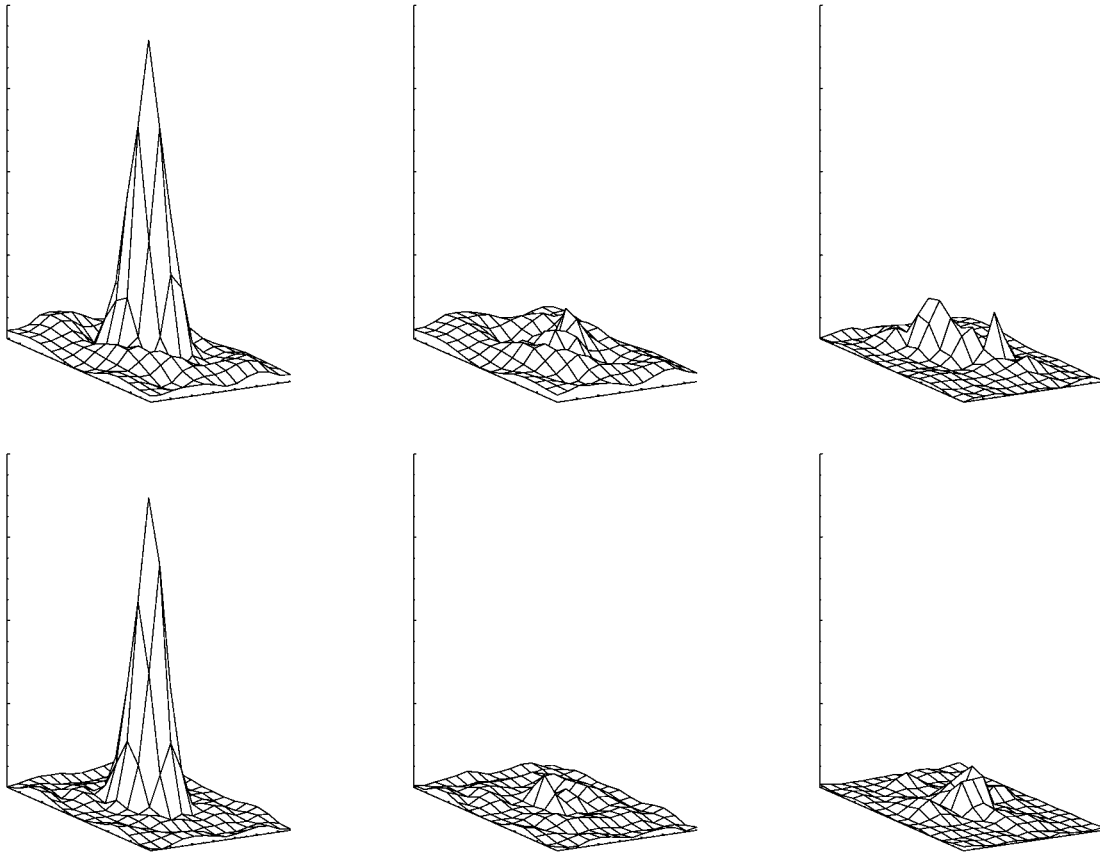


FIG. 4.—HIREs beam absolute differences. The top row shows the absolute difference between the normalized $100\ \mu\text{m}$ and $12\ \mu\text{m}$ beams located at $l = 189^\circ$, $b = 3^\circ$. The bottom row shows the results for the irregular beams located at $l = 93^\circ$, $b = +4^\circ$. The differences for regular HIREs beams, the new convolution technique, and cross-band simulation are shown from left to right. All of the surface plots are at the same scale. The beam images have been subsampled by a factor of 3 for clarity.

would repeat the technique for a number of fields and then mosaic the images together. In a standard 1.4×1.4 field, beam information is reported in a 7×7 array of points spread evenly over the image. This sampling interval greatly undersamples the beam variation across the image, but finer sampling was not possible because of the way the beam maps are constructed. The algorithm assumes that the beam information describes the beam shape over the 0.2×0.2 region surrounding each beam. The validity of this assumption depends upon how little the scan pattern changes over the 0.2×0.2 . Users can determine this by looking at either the beam maps or the detector track maps that are included in the standard MIGA and IGA releases and in a typical HIREs request.

The algorithm runs as follows. To start, one has two images, image 1 and image 2, at *IRAS* band 1 and band 2, respectively. The major and minor FWHM and orientation for the beams in image 2 is read from a file the user has prepared from the HIREs beam tables. For each beam a two-dimensional Gaussian kernel is created and convolved with a 0.4×0.4 region centered on that beam that has been clipped out of image 1.

The size of the area clipped out was chosen to provide ample room to avoid edge effects when doing the convolution. The 0.2×0.2 center of the convolved region is clipped out and placed in the final convolved image. The procedure is repeated until all 25 beams in the 1° center of the image have been processed and the $1^\circ \times 1^\circ$ convolved image has been built up. Beams centered 0.1 from the outer edge of the image are ignored since they correspond to a 0.2 border that should be clipped off the final images before mosaicking or making ratio maps (this buffer zone was included in the HIREs processing to avoid problems with artificially low detector coverage). The entire procedure is then repeated using image 2 and the beam data for image 1.

Essentially the new algorithm is a combination of the smoothing technique discussed in § 2.2 and the cross-band simulator technique described in § 2.4. However, instead of scanning the image with the *IRAS* beam shape and detector scan pattern, it uses a two-dimensional Gaussian convolution to match the beam shapes based upon the information provided in the beam maps and tables. Also, instead of smoothing to a

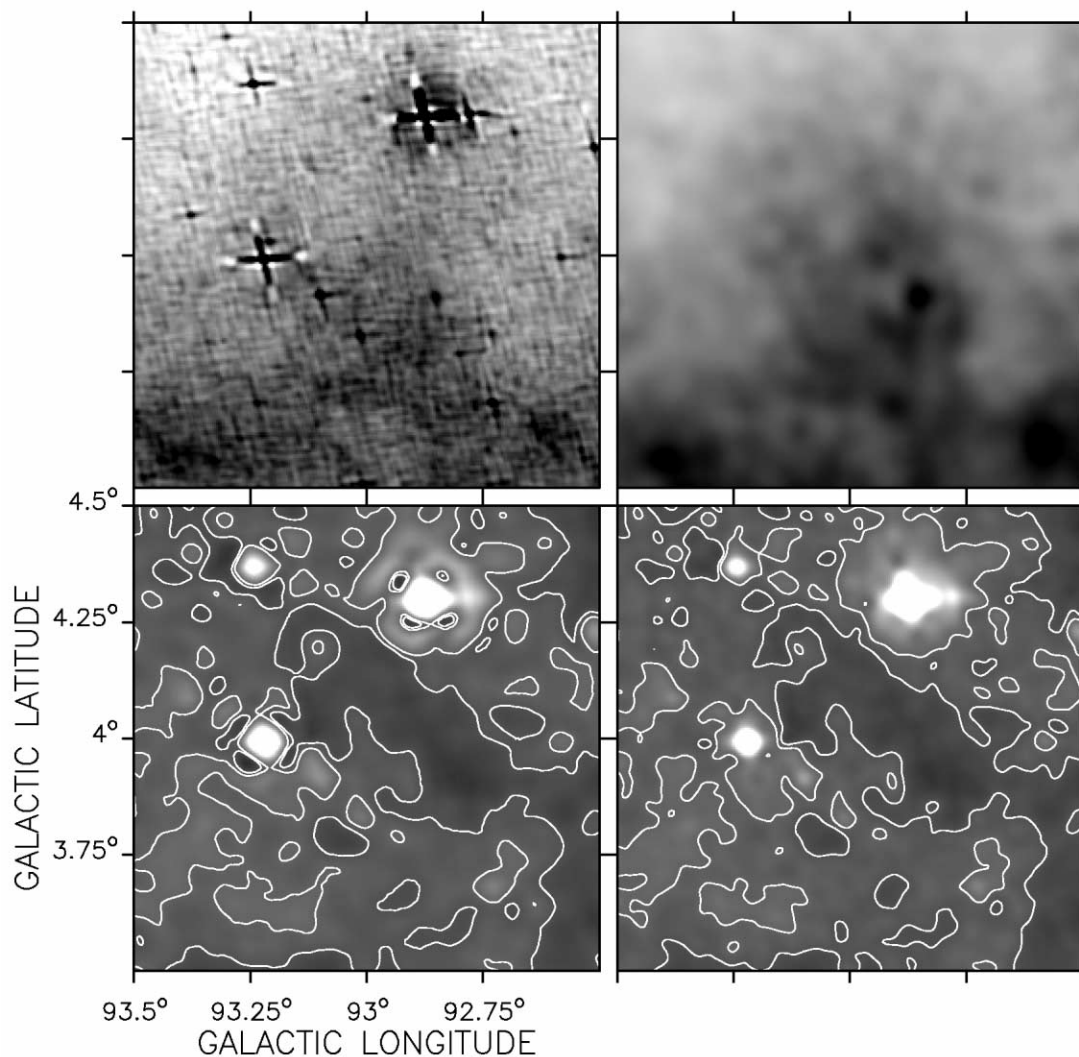


FIG. 5.—High ecliptic latitude region. Figure shows a comparison of ratio maps ($12\ \mu\text{m}/100\ \mu\text{m}$) constructed using the HIRES simulator (*bottom left*) and using the convolution technique (*bottom right*) for a region with a HIRES beam with cross-shaped wings (linear gray scale from 0.03 to 0.09, *black to white*, with contours at 0.049 and 0.053). The top row shows the original HIRES images at $12\ \mu\text{m}$ (*left*; linear gray scale from 3 to $7\ \text{MJy sr}^{-1}$, *white to black*) and $100\ \mu\text{m}$ (*right*; linear gray scale from 50 to $135\ \text{MJy sr}^{-1}$, *white to black*).

markedly lower resolution, it convolves the image only to the degree necessary to match the two images. The algorithm was implemented using IDL because of its matrix manipulation capability but could easily be modified to any computer language.⁶

While this algorithm was developed for and initially applied to *IRAS* HIRES data, there is nothing about it that restricts its use solely to infrared data. The algorithm could be easily applied to, for example, an infrared and a radio data set provided sufficient information about the beam shapes was available (see § 5). Large-scale radio spectral index maps can also be created using the algorithm. A specialized version of the algorithm

(called MOSCONV, for MOSaic CONVolve) has been developed independently by L. Higgs at Dominion Radio Astrophysical Observatory to create large-scale ($\sim 5^\circ \times 5^\circ$) spectral index maps using the 1420 MHz and 408 MHz data and ancillary files contained in the CGPS.

4. TESTS AND COMPARISONS

The algorithm was tested on two regions with markedly different HIRES beam shapes. In each case, three sets of images and beam maps were created: regular HIRES, cross-band simulated HIRES, and HIRES processed with the new algorithm. The images allowed us to compare the relative quality of the resulting ratio maps, while the beam maps allowed us to com-

⁶ IDL code is available from C. R. K. upon request.

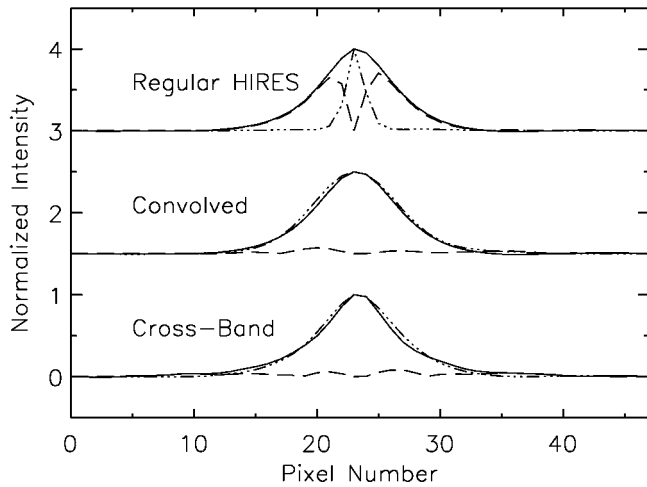


FIG. 6.—High ecliptic latitude HIRES beam comparison. Same as Fig. 3, but for HIRES beams located at $l = 93^{\circ}0$, $b = +4^{\circ}0$.

pare in more detail how the beam shape changes in each case. For the beam comparisons, we focused on the 12 and 100 μm HIRES beams since they have the greatest difference in resolution and beam shape.

First we looked at a field (centered at $l = 189^{\circ}0$, $b = 3^{\circ}0$ near IC 443; see Fig. 2) where the HIRES beam is “regular”; i.e., it is very close to a two-dimensional Gaussian.

Figure 3 shows one-dimensional cuts through the minor axis (at the same position angle) of the 12 and 100 μm beams located at $l = 189^{\circ}0$, $b = 3^{\circ}0$ along with the absolute value of the difference between the two beams. The beam profiles have been normalized to the same central intensity so that differences in the beam shapes can be highlighted. Notice the large difference in the beam shapes in the raw images (top profile in Fig. 3). Negative rings are evident in the 100 μm beam; this is a well known artifact of HIRES processing (Cao et al. 1997). The middle profiles show the beams that are created using the algorithm presented in this paper. The match between the beams is greatly improved from the original images. Finally the lower cuts show the beams that are formed in the cross-band simulation process. There is a significant improvement over the regular HIRES beams, and even the ringing around the center of the beam is well matched in this case.

To illustrate the quality of the match in two dimensions, the upper row of Figure 4 shows surface plots of the absolute difference between the 12 and 100 μm beams for the regular HIRES, convolution, and cross-band simulation processes for this region. Again there is a substantial, comparable improvement in the match between the beams evident in the convolution and cross-band simulation plots. The differences between the two beams for the cross-band simulation and convolution beams are of the same (small) magnitude.

The same tests were repeated in another field (centered

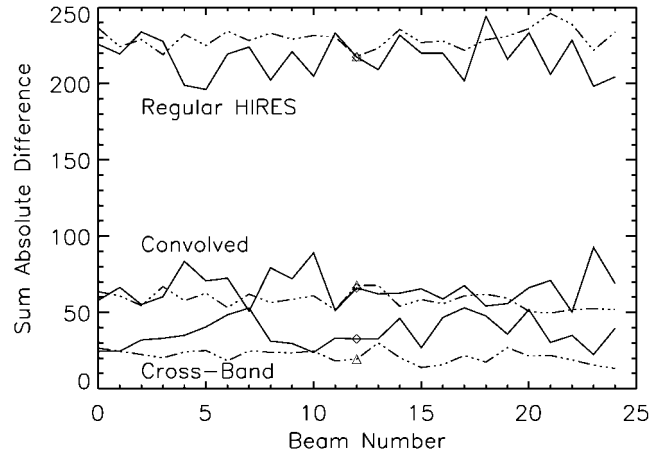


FIG. 7.—The sum of the absolute difference between the 12 and 100 μm beams for all of beams in the two areas examined in this paper. The solid line is for the regularly shaped beams, and the dot-dashed line is for the high ecliptic latitude beams that have cross-shaped wings. The symbols indicate the beams that were used for the detailed comparisons shown in Figs. 3, 4, and 6.

at $l = 93^{\circ}0$, $b = 4^{\circ}0$; see Fig. 5) where the HIRES beam has X-shaped wings (especially evident at 12 μm). The one-dimensional cuts through the various beams are shown in Figure 6. Again we see a significant comparable improvement in the agreement between the beam shapes both in the cross-band simulation and our new technique. The bottom row of Figure 4 shows the surface plots of the difference in the beam shape. These plots show that the convolution and cross-band simulation technique will provide similar degrees of improvement to the quality of the beam match.

Figure 7 shows the sum of the absolute difference between the 12 μm and 100 μm beams for all of the beams in the two areas we tested. The beam that has been discussed in detail is indicated on the figure and clearly is a representative result. In all cases we see that the convolution algorithm yields a substantial improvement in the match between the two beams that is comparable to the results obtained using the cross-band simulation technique.

The resulting ratio maps created using our convolution technique and the cross-band simulation technique are shown in the bottom two frames of Figures 2 and 5. The only major difference between the two results is the detailed structure close to the point sources. The convolution map is much faster to create than the cross-band simulation map and results in a final ratio map that is comparable in achieved resolution and overall image quality.

In order to compare the various ratio maps, the rms fractional difference between the cross-band simulated and the unprocessed HIRES or convolution ratio image was calculated. This was also carried out for four subregions corresponding to various features in each image. Results from the comparison are

TABLE 1
 RATIO IMAGE COMPARISON: REGULAR BEAM

IMAGE ^a	rms FRACTIONAL DIFFERENCE				
	Area 1	Area 2	Area 3	Area 4	All
RAW-SIM					
b1/b2	0.075	0.078	0.096	0.065	0.080
b1/b3	0.084	0.139	0.162	0.094	0.100
b1/b4	0.088	0.232	0.247	0.110	0.130
b2/b3	0.061	0.074	0.128	0.105	0.085
b2/b4	0.058	0.077	0.112	0.077	0.090
b3/b4	0.042	0.047	0.150	0.090	0.072
CON-SIM					
b1/b2	0.041	0.050	0.064	0.040	0.049
b1/b3	0.033	0.067	0.078	0.073	0.079
b1/b4	0.013	0.056	0.061	0.071	0.098
b2/b3	0.032	0.049	0.094	0.084	0.055
b2/b4	0.013	0.030	0.051	0.057	0.044
b3/b4	0.021	0.023	0.074	0.057	0.038

NOTE—RAW: no special processing. CON: convolution technique. SIM: cross-band simulation. Area 1: featureless. Area 2: around point source visible at 12, 25, and 60 μm . Area 3: around very bright point source visible at 12, 25, and 60 μm . Area 4: around point source visible in all bands. All: entire image.

^a b1: 12 μm ; b2: 25 μm ; b3: 60 μm ; b4: 100 μm .

 TABLE 2
 RATIO IMAGE COMPARISON: IRREGULAR BEAM

IMAGE ^a	rms FRACTIONAL DIFFERENCE				
	Area 1	Area 2	Area 3	Area 4	All
RAW-SIM					
b1/b2	0.030	0.109	0.191	0.030	0.060
b1/b3	0.038	0.161	0.280	0.043	0.087
b1/b4	0.046	0.305	0.431	0.058	0.131
b2/b3	0.020	0.093	0.247	0.030	0.054
b2/b4	0.022	0.165	0.396	0.034	0.085
b3/b4	0.017	0.025	0.138	0.065	0.032
CON-SIM					
b1/b2	0.016	0.089	0.139	0.015	0.041
b1/b3	0.012	0.085	0.272	0.021	0.055
b1/b4	0.010	0.074	0.241	0.016	0.049
b2/b3	0.010	0.035	0.192	0.022	0.037
b2/b4	0.007	0.032	0.160	0.015	0.031
b3/b4	0.007	0.008	0.044	0.017	0.011

NOTE.—RAW: no special processing. CON: convolution technique. SIM: cross-band simulation. Area 1: featureless. Area 2: around point source visible at 12, 25, and 60 μm . Area 3: around very bright point source visible at 12, 25, and 60 μm . Area 4: around point source visible in all bands. All: entire image.

^a b1: 12 μm ; b2: 25 μm ; b3: 60 μm ; b4: 100 μm .

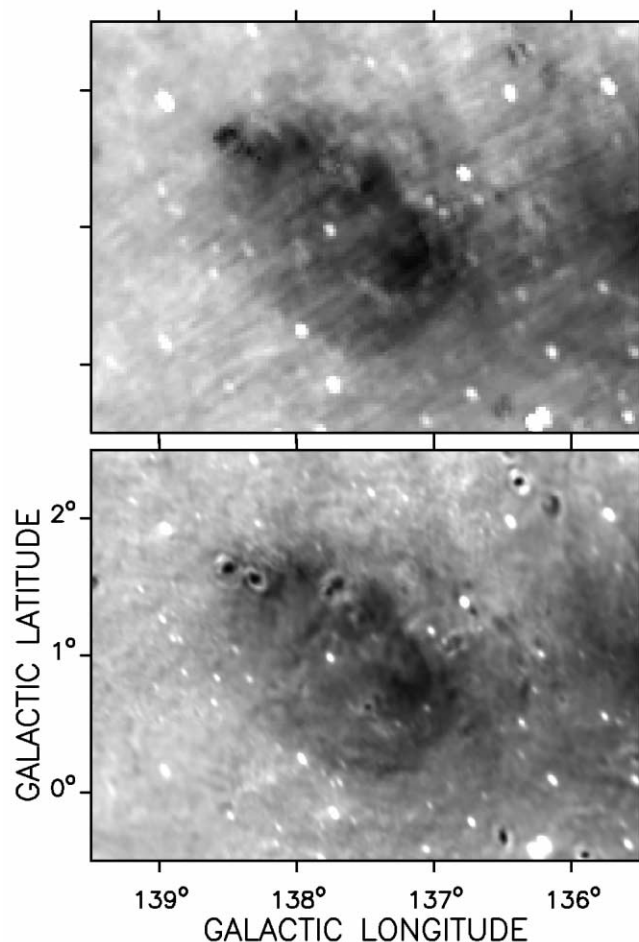


FIG. 8.—W5 12 $\mu\text{m}/100 \mu\text{m}$ ratio maps. Upper ratio map was constructed using ISSA images; lower ratio map was created using IGA and MIGA images processed with the algorithm described in this paper. Both maps are linearly stretched from 0.02 to 0.08 (black to white). Note the significant improvement in the image quality obtained by using the IGA and MIGA images. Dark areas (both extended and point source) correspond to regions of ionized gas where PAH grains are destroyed by the hard UV radiation field.

presented in Tables 1 and 2 for various *IRAS* band combinations. As would be expected, the convolved ratio map is a much better match to the simulated ratio map, as indicated by the lowering of the rms fractional difference for all of the various *IRAS* band combinations. This quantitative assessment was combined with a visual inspection of the convolved ratio images and the simulated ratio images to make sure they were comparable overall.

5. SAMPLE APPLICATIONS

In Figure 8 we show an example of how this technique can be applied to the creation of large-scale infrared ratio maps. The upper image is the 12 $\mu\text{m}/100 \mu\text{m}$ ratio map of the W5 H II region created using ISSA images. The poor resolution

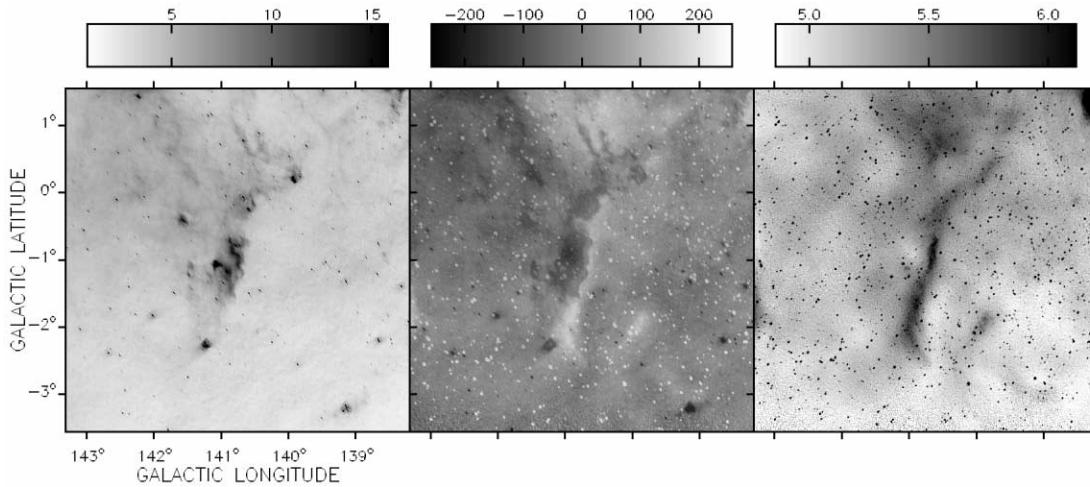


FIG. 9.—Large-scale multiwavelength comparison. A $5^{\circ}12 \times 5^{\circ}12$ mosaic from the CGPS database centered on $l = 140^{\circ}75, b = -1^{\circ}0$. The left and right panels show the original $12 \mu\text{m}$ (MJy sr^{-1}) and 1420 MHz (K) continuum emission mosaics, respectively. The middle panel shows the result of scaling the beam-matched images from 0 to 256 and subtracting the infrared image from the radio image.

and image quality (striping) referred to in § 1 are apparent. The lower image is the same image constructed using HIRES data from the IGA and MIGA processed using our algorithm to match the 12 and $100 \mu\text{m}$ beam shape at all locations in the image. Clearly this image is more useful for any scientific investigation.

The region with a low $12 \mu\text{m}/100 \mu\text{m}$ ratio that dominates the center of the map corresponds to the ionized gas in W5. The drop in this ratio relates to the destruction of polycyclic aromatic hydrocarbon (PAH) dust grains in the ionized regions

which in turn causes a reduction in the $12 \mu\text{m}$ emission. The various dark points visible in this map are all H II regions as confirmed by inspection of the 1420 MHz continuum images in the CGPS database. Maps like this one can be easily compared with large-scale data products at other wavelengths in order to investigate the properties of interstellar dust in different environments. Note that whenever anything unusual is found in a HIRES color map, no matter how the map was created, a detailed examination of the separate-band images is called for (e.g., aperture photometry, checking the noise and coverage maps, etc.).

Although we have focused on the construction of infrared ratio maps in this paper, another application of the new algorithm is the comparison of multiwavelength data sets using difference images or multicolor imaging. In these applications the two data sets are first scaled and then either subtracted or displayed as different colors. This allows the relative distribution of the emission to be easily studied.

Figure 9 shows two of the typical $5^{\circ}12 \times 5^{\circ}12$ mosaics from the CGPS database in the infrared ($12 \mu\text{m}$ HIRES; left panel) and in 1420 MHz continuum (right panel). The object that dominates the center of the mosaic is LBN $140.77-1.42$. Comparison with CO and H I images of this region in the CGPS database shows that this region is an edge-on view of an H II+H I+molecular gas interface (a photodissociation region, or PDR). We were interested in investigating the relative position of the $12 \mu\text{m}$ emission and the 1420 MHz continuum emission at this interface. The beam shape in the 1420 MHz mosaic is also variable across the mosaic, so we created beam-matched images using the beam information provided in the CGPS database and the algorithm presented in this paper. Lower and upper data limits (peak 95% of image histogram) were selected that resulted in similar visual contrast in each

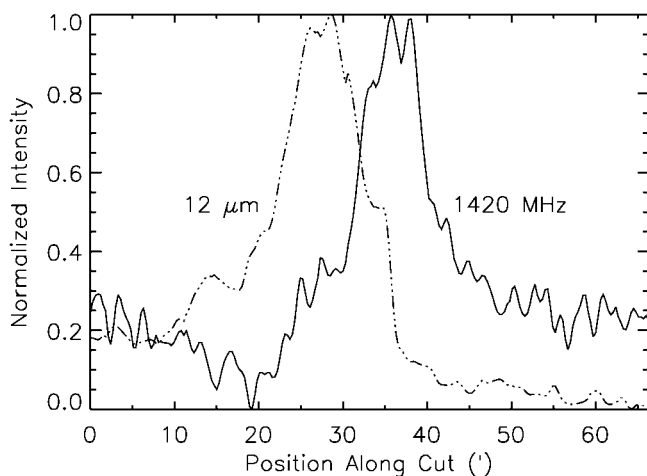


FIG. 10.—Infrared and radio continuum emission through the PDR LBN $140.77-1.42$ (from $l = 141^{\circ}255, b = -0^{\circ}860$ to $l = 140^{\circ}130, b = -0^{\circ}965$; $18''$ wide; beam $\sim 1'$). The $\sim 1^{\circ}$ long slice was taken from beam-matched versions of the images shown in Fig. 9. Note the offset in the infrared and radio emission peaks and the sharp increase in the infrared emission followed by a more gradual decline.

image (as shown in Fig. 9). Each image was then rescaled from 0 to 256 and the $12\ \mu\text{m}$ image was subtracted from the 1420 MHz continuum image. The center panel of Figure 9 shows the resulting difference map. Dark areas are regions where the IR emission dominates; light areas are where 1420 MHz continuum emission dominates. Instead of subtracting the images, one could also construct a two-color image with the infrared data in the red channel and radio in the blue channel (for example). In this case, we see that the intense $12\ \mu\text{m}$ emission is coming mostly from a region just to the east of the intense continuum emission with a very slight overlap area. The PDR nature of the object is best seen by examining a cut through the region from east to west. Figure 10 shows a cut (background subtracted and normalized) from $l = 141^\circ 255$, $b = -0^\circ 860$ to $l = 140^\circ 130$, $b = -0^\circ 965$. The $12\ \mu\text{m}$ emission peaks just inside of the 1420 MHz emission and then falls off in intensity as one moves farther into the neutral/molecular material to the east. This rapid increase in infrared emission at the ionized-neutral interface followed by a slow decline in emission as one moves into the neutral/molecular material is what one expects to see in a cross section of a PDR (Teilens et al. 1993).

6. CONCLUSIONS

Beam-matched maps of HIRES *IRAS* data products have been shown to be useful both in studies of dust properties and

in multiwavelength analyses of the dust and gas phases of the interstellar medium.

For images in any of the *IRAS* bands, simple ratio maps are seldom sufficient for any application beyond superficial inspection. For quantitative studies involving HIRES data, some degree of extra processing is required.

To create high-resolution infrared beam-matched maps, a simple, fast, convolution technique that makes full use of the beam shape information reported in the MIGA and IGA releases and also available as part of the standard HIRES request output has been developed. The algorithm provides a good match of the HIRES beams combined with a minimal loss of the resolution gained from using the HIRES processing technique.

We expect that this technique will be quite useful for the creation of very large-scale (many square degree) infrared ratio maps for studies of the properties of dust in the ISM. The technique is also useful for the construction of multiwavelength difference or multicolor images and large-scale radio spectral index maps.

C. R. K. would like to thank the Ontario Graduate Scholarship program for financial support during part of this study. The research of P. G. M. is supported through grants from the Natural Sciences and Engineering Research Council of Canada (NSERC).

REFERENCES

- Aumann, H. H., Fowler, J. W., & Melnyk, M. 1990, *AJ*, 99, 1674
 Boulanger, F., Falgarone, E., Puget, J.-L., & Helou, G. 1990, *ApJ*, 364, 136
 Cao, Y., Prince, T. A., Terebey, S., & Beichman, C. 1996, *PASP*, 108, 535
 Cao, Y., Terebey, S., Prince, T. A., & Beichman, C. 1997, *ApJS*, 111, 387
 Fowler, J. W. & Aumann, H. H. 1994, in *Science with High Spatial Resolution Far Infrared Data*, ed. S. Terebey & J. Mazzarella (Publ. 94-5; Pasadena: JPL), 1
 Helou, G., Ryter, C., & Soifer, B. T. 1991, *ApJ*, 376, 505
IRAS Catalogs and Atlases: Explanatory Supplement. 1988, ed. C. A. Beichman, G. Neugebauer, H. J. Habing, P. E. Clegg, & T. E. Chester (Washington, DC: GPO)
 Kerton, C. R., & Martin, P. G. 2000, *ApJS*, 126, 85
 Ryter, C., Puget, J.-L., & Pérault, M. 1987, *A&A*, 186, 312
 Taylor, A. R. 1999, in *ASP Conf. Ser. 168, New Perspectives on the Interstellar Medium*, ed. A. R. Taylor, T. L. Landecker, & G. Joncas (San Francisco: ASP), 3
 Tielens, A. G. G. M., Meixner, M. M., van der Werf, P. P., Bregman, J., Tauber, J. A., Stutzki, J., & Rank, D. 1993, *Science*, 262, 86
 Wang, Z. 1994, in *ASP Conf. Ser. 58, The First Symposium of the Infrared Cirrus and Diffuse Interstellar Clouds*, ed. R. M. Cutri & W. B. Latter (San Francisco: ASP), 416
 Wheelock, S. L., et al. 1994, *IRAS Sky Survey Atlas Explanatory Supplement* (Publ. 94-11; Pasadena: JPL)
 Xu, C., & Helou, G. 1996, *ApJ*, 456, 152